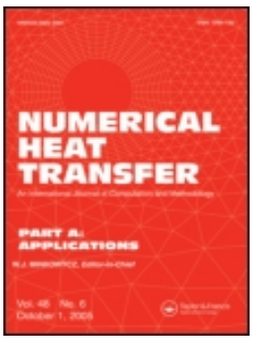

Taylor & Francis
Taylor & Francis Group

Numerical Heat Transfer: Part A: Applications

ISSN: 1040-7782 (Print) 1521-0634 (Online) Journal homepage: https://www.tandfonline.com/loi/unht20

# NUMERICAL SIMULATION OF THREE-DIMENSIONAL LAMINAR, SQUARE TWIN-JET IMPINGEMENT ON A FLAT PLATE, FLOW STRUCTURE, AND HEAT TRANSFER

L. B. Y. Aldabbagh & I. Sezai

**To cite this article:** L. B. Y. Aldabbagh & I. Sezai (2002) NUMERICAL SIMULATION OF THREE-DIMENSIONAL LAMINAR, SQUARE TWIN-JET IMPINGEMENT ON A FLAT PLATE, FLOW STRUCTURE, AND HEAT TRANSFER, Numerical Heat Transfer: Part A: Applications, 41:8, 835-850, DOI: 10.1080/10407780290059378

**To link to this article:** https://doi.org/10.1080/10407780290059378

Published online: 30 Nov 2010.

Submit your article to this journal

Article views: 223

View related articles

Citing articles: 1 View citing articles

Full Terms & Conditions of access and use can be found at
https://www.tandfonline.com/action/journalInformation?journalCode=unht20

Numerical Heat Transfer, Part A, 41: 835–850, 2002
Copyright © 2002 Taylor & Francis
1040-7782/02 $12.00 + .00
DOI: 10.1080/1040778029005937 8

# NUMERICAL SIMULATION OF THREE-DIMENSIONAL LAMINAR, SQUARE TWIN-JET IMPINGEMENT ON A FLAT PLATE, FLOW STRUCTURE, AND HEAT TRANSFER

***L. B. Y. Aldabbagh and I. Sezai***
*Mechanical Engineering Department, Eastern Mediterranean University, Magosa, Mersin, Turkey*

***The flow and heat transfer characteristics of impinging laminar square twin jets have been investigated numerically through the solution of three-dimensional Navier–Stokes and energy equations in a steady state. The simulations have been carried out for jet-to-jet spacings of 4, 6, and 8 and for nozzle-exit-to-plate distances between 0.25D and 5D. The calculated results show that the flow structure of square twin jets impinging on a heated plate is strongly affected by the jet-to-plate distance. In addition, for very small jet-to-plate distances ($L_z \approx 0.25D$), no upwash fountain flow can form at the collision point where the jets are merely diverted in the transverse direction. For such nozzle-to-plate distances the wall jet fills the whole gap between the plates with no vortex motion around the twin jets.***

## INTRODUCTION

Impinging jets are extensively used in diverse industrial applications because of their highly attractive local heat and mass transfer characteristics. Industrial applications include tempering of glass, drying of paper and textiles, annealing of nonferrous metal sheets, and cooling of microelectronic components. Although such jets yield very high heat transfer coefficients in the stagnation zone, the cooling performance drops rapidly away from the impingement zone. For this reason jets are often used in arrays in industrial practice. In such cases the interaction between the jets in the array plays an important role in the cooling performance. The collision of the wall jets after impingement produces a rather complex flow field. To gain further understanding of jet-to-jet interaction, the analysis can be confined to only two such jets. Therefore, study of a three-dimensional impinging twin-jet flow may provide some basic understanding of the practical three-dimensional multiple-jets flow field.

The experimental and theoretical investigations of jets are mostly related to turbulent jets. Although many applications involve turbulent jets, laminar jets are also encountered when the fluid is highly viscous or the geometry is miniature, as in microelectronics. Numerous studies have been reported in the literature on the flow, heat, and mass transfer distributions under single laminar impinging jets (Heiningen

Received 1 March 2001; accepted 26 October 2001.
Address correspondence to I. Sezai, Department of Mechanical Engineering, Eastern Mediterranean University, Magos, Mersin 10, Turkey. E-mail: ibrahim.sezai@emu.edu.tr

## NOMENCLATURE

| | | | |
|---|---|---|---|
| $A_x, A_y, A_z$ | aspect ratios in $x$, $y$, and $z$ direction, $L_x/D$, $L_y/D$, $L_z/D$ | $u_j$ | jet exit velocity (m/s) |
| | | $U$ | nondimensional Cartesian velocity, in $x$-direction ($u/u_j$) |
| $D$ | jet width | | |
| $h$ | heat transfer coefficient ($W/m^2K$) | $V$ | nondimensional Cartesian velocity, in $y$-direction ($v/u_j$) |
| $k$ | thermal conductivity (W/m K) | | |
| $L_x$ | length of heated surface, in $x$-direction (m) | $W$ | nondimensional Cartesian velocity, in $z$-direction ($w/u_j$) |
| $L_y$ | length of heated surface, in $y$-direction (m) | $X_n$ | jet-jet spacing |
| | | $X, Y, Z$ | nondimensional Cartesian coordinates, $x/D$, $y/D$, $z/D$, respectively |
| $L_z$ | distance from jet exit to impingement plate (m) | | |
| Nu | local Nusselt number, ($hD/k$) | $x, y, z$ | Cartesian coordinates |
| $p$ | pressure | $\alpha$ | thermal diffusivity ($m^2/s$) |
| $P$ | nondimensional pressure ($p/\rho u_j^2$) | $\nu$ | kinematic viscosity ($m^2/s$) |
| Pr | Prandtl number ($\nu/\alpha$) | $\rho$ | density ($kg/m^3$) |
| $q''_w$ | local convective heat flux | $\phi$ | $U$, $V$, $W$, $P$, or $T$ field |
| Re | jet Reynolds number ($u_j D/\nu$) | | |
| $t$ | temperature | | |
| $T$ | nondimensional temperature, $(t - t_j)/(t_w - t_j)$ | **Subscripts** | |
| | | $j$ | jet exit |
| $u, v, w$ | Cartesian velocities | $w$ | wall |

et al. [1], Chou and Hung [2], Mikhail et al. [3], Yuan et al. [4], Schafer et al. [5], Wadsworth and Mudawar [6], and Sezai and Mohamad [7]).

The effects of interaction between twin planar free-surface jets have been studied experimentally by Slayzak et al. [8] using water as the working fluid. The emphasis was placed on the secondary stagnation point associated with the interaction between the opposing wall jets, characterized by an upwash fountain. It was found that interacting wall jets yielded a strong upwelling of the upwash fountain, beneath which convection coefficients were comparable with those associated with the jet impingement regions. The impingement of confined single and twin turbulent jets though a crossflow was studied by Barata et al. [9]. The experiments were performed using laser-doppler measurements for the jet exit 5 jet diameters above the ground plate. In addition, a three-dimensional numerical model was used to predict the flow field, produced by twin jets. The results have shown large penetration of the impinging jets, which exhibit a similar pattern for single and twin-jet configurations. A two-dimensional numerical model was used by Chuang et al. [10] to determine the flow characteristics associated with an unsteady, compressible impinging twin slot jet between two plates. The calculated results show that several recirculating zones are distributed around the flow field. Their size and location are closely related to the jet exit height above the ground, the nozzle spacing, and the strength of cross flow. In addition, a fountain upwash flow occurs between the nozzles, and two low-pressure recirculating zones are induced by the interaction between the nozzle mainstream and the fountain upwash flow. The three-dimensional turbulent impinging square twin jet with no crossflow is analyzed by Chuang and Nieh [11] using the PHOENICS code. The calculated results show that the size and location of the recirculating zones around the jets are different from the two-dimensional flow field due to the effect of flow stretching in the transverse direction. The experimental

investigation of Siclari et al. [12] is focused on the stagnation line and upwash formation in two impinging jets.

There is a considerable body of literature dealing with flow and heat transfer in arrays of jets (Metzger et al. [13], Hollworth and Dagan [14], Kim and Benson [15], Huber and Viskanta [16], Barata [17], Garrett and Webb [18], Tzeng et al. [19]). These investigations have focused largely on arrays for which cross-flow effects degrade the high stagnation heat transfer and the effect of the geometric arrangement of jets. The study of Seyedein et al. [20] is aimed to investigate the effect of confinement surface inclination on the degree of nonuniformity in multijet impingement, by using a two-dimensional, laminar numerical model.

This work deals with laminar, three-dimensional analysis of a square twin jet impinging on a heated flat surface (Figure 1). The structure of the flow field and its effect on heat transfer is investigated numerically. Our results show that at very small nozzle-to-impingement-plate distances ($L_z \approx 0.25D$) no upwash fountain can form at the collision point of the two jets. For such small nozzle-to-plate distances the wall jets fill the whole plate-to-plate spacing with no vortex motion around the jets.

## COMPUTATION SCHEME

The steady state, three-dimensional Navier–Stokes and energy equations for incompressible flows in Cartesian coordinates are used for this study. The velocity and length are normalized with jet-exit velocity and jet width, respectively. The buoyancy effect has been neglected. Hence this study is valid for a Richardson number less than 1.

The nondimensional continuity, momentum, and energy equations for laminar flows with constant properties can be written as

$$\frac{\partial U}{\partial X} + \frac{\partial V}{\partial Y} + \frac{\partial W}{\partial Z} = 0 \tag{1}$$

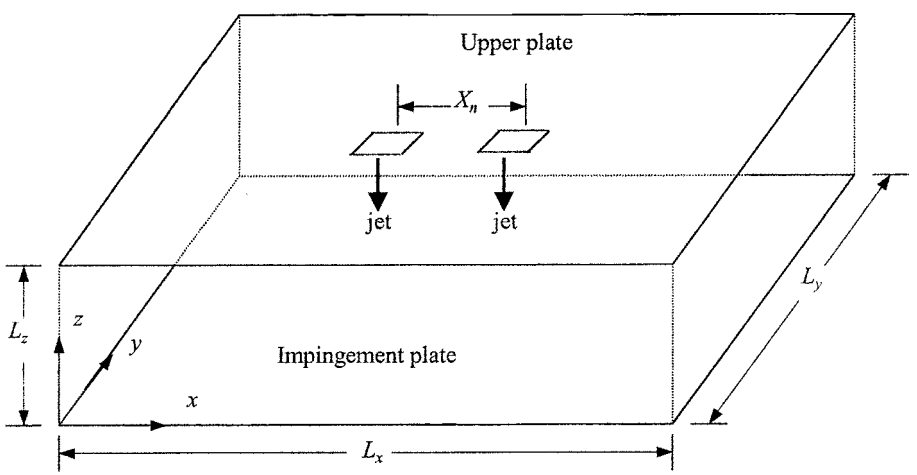


**Figure 1.** Definitions of geometric parameters and the coordinate system.

$$U\frac{\partial U}{\partial X}+V\frac{\partial U}{\partial Y}+W\frac{\partial U}{\partial Z}=-\frac{\partial P}{\partial X}+\frac{1}{\mathrm{Re}}\nabla^2 U \tag{2}$$

$$U\frac{\partial V}{\partial X}+V\frac{\partial V}{\partial Y}+W\frac{\partial V}{\partial Z}=-\frac{\partial P}{\partial Y}+\frac{1}{\mathrm{Re}}\nabla^2 V \tag{3}$$

$$U\frac{\partial W}{\partial X}+V\frac{\partial W}{\partial Y}+W\frac{\partial W}{\partial Z}=-\frac{\partial P}{\partial Z}+\frac{1}{\mathrm{Re}}\nabla^2 W \tag{4}$$

$$U\frac{\partial T}{\partial X}+V\frac{\partial T}{\partial Y}+W\frac{\partial T}{\partial Z}=\frac{1}{\mathrm{Re}\,\mathrm{Pr}}\nabla^2 T \tag{5}$$

The boundary conditions for velocities are as follows:

$$\frac{\partial U}{\partial X}=\frac{\partial V}{\partial X}=\frac{\partial W}{\partial X}=0 \quad \text{at } X=0 \quad X=A_x$$

$$\frac{\partial U}{\partial Y}=\frac{\partial V}{\partial Y}=\frac{\partial W}{\partial Y}=0 \quad \text{at } Y=0 \quad Y=A_y$$

$$U=V=W=0 \text{ at } Z=0, Z=A_z \text{ except at nozzles exit}$$

$$U=V=0 \quad W=-1 \quad \text{at nozzle exit}$$

The boundary conditions for temperature are

$$\text{At } X=0 \quad \frac{\partial T}{\partial X}=0 \quad \text{for } U<0$$

$$T=0 \quad \text{for } U>0$$

$$\text{At } X=A_x \quad \frac{\partial T}{\partial X}=0 \quad \text{for } U>0$$

$$T=0 \quad \text{for } U<0$$

$$\text{At } Y=0 \quad \frac{\partial T}{\partial Y}=0 \quad \text{for } V<0$$

$$T=0 \quad \text{for } V>0$$

$$\text{At } Y=A_y \quad \frac{\partial T}{\partial Y}=0 \quad \text{for } V>0$$

$$T=0 \quad \text{for } V<0$$

$$\text{At } Z=0 \quad T=1$$

$$\text{At } Z=A_z \quad \frac{\partial T}{\partial Z}=0 \quad \text{except at nozzle's exit}$$

$$T=0 \quad \text{at nozzle exit.}$$

## METHOD OF SOLUTION

The governing equations are discretized by using the finite volume method in staggered, nonuniform grids. The grids are generated such that denser grid clustering is obtained at the edges of the jets-exit cross section in the $x$- and $y$-directions. The grid size at the nozzle cross sections is uniform. The maximum difference between the results obtained by using $201 \times 201 \times 47$ and $151 \times 151 \times 35$ grids is 4.15% for the local Nusselt number and 0.75% for the vertical velocity distribution. The corresponding differences between $151 \times 151 \times 35$ and $101 \times 101 \times 25$ grids is 12.27% and 1.67%. Hence, all calculations are performed with $151 \times 151 \times 35$ grids. For the cases of $A_z = 0.25$ and 1.0 the solution domain has $L_x = L_y = 35D$. For $A_z > 1$ the solution domain in $x$- and $y$-directions is extended to $100D$ and grid clustering is adjusted to have a similar grid distribution around the impingement region for different domain sizes. In the $z$-direction a sine function distribution is employed, yielding denser grids near the top and near the impingement plate. The QUICK scheme (Leonard [21]) with ULTRA-SHARP flux limiting strategy (Leonard and Mokhtari [22]; Leonard and Drummond [23]) was used to calculate the convection of a scalar term ($\phi$) at a control volume face. The extra neighboring points resulting from the application of the QUICK scheme are written as the sum of the upwind face value plus a correction term involving the values from the previous iteration. The correction term is added to the source term in accordance with a deferred correction procedure (Leonard and Drummond [23]) so that the numerical stability is increased, while keeping the seven diagonal structures of the coefficient matrix. The BICGSTAB (Van der Vorst [24]) iterative method with SSOR preconditioning (Saad [25]) is applied to the pressure and energy equations in the sequential procedure of the SIMPLEC (Van Doormaal and Raithby [26]) algorithm. An under-relaxation factor of 0.8 for Re = 100 and 0.7 for Re = 300 and 500 is used for momentum and energy equations in all calculations. Iterations are continued until the second norm of the residuals for all equations are reduced below $10^{-6}$, where no significant variations are observed at this residual level.

## RESULTS AND DISCUSSIONS

Air is used as the working fluid having a Prandtl number of 0.71. The analysis is performed for the following aspect ratios, $A_z$: 0.25, 1, 2, 3, 4, and 5. Center-to-center distance values between the jets used are $4D$, $6D$, and $8D$. The cross section of the nozzles is taken to be square, and the velocity distribution at the exit of the nozzles is assumed to have a flat profile.

### Flow Structure

Figure 2*a* shows the stream traces of the predicted velocity field on the mid-vertical $x$-$z$ plane, for a plate-to-plate distance of 5 jet widths. The stream traces are obtained from the $U$-$W$ data on the corresponding plane. At the impingement plane two wall jets are formed spreading in the radial direction. An upwash fountain flow is formed in the center of the two impinging jets due to the collision of the two individual jets. As soon as the jets exit from the nozzle, a negative pressure is induced around each, which drags fluid from the surrounding. As a result, fluid is entrained in the flow, forming a vortex on the periphery of each jet. The peripheral vortex is

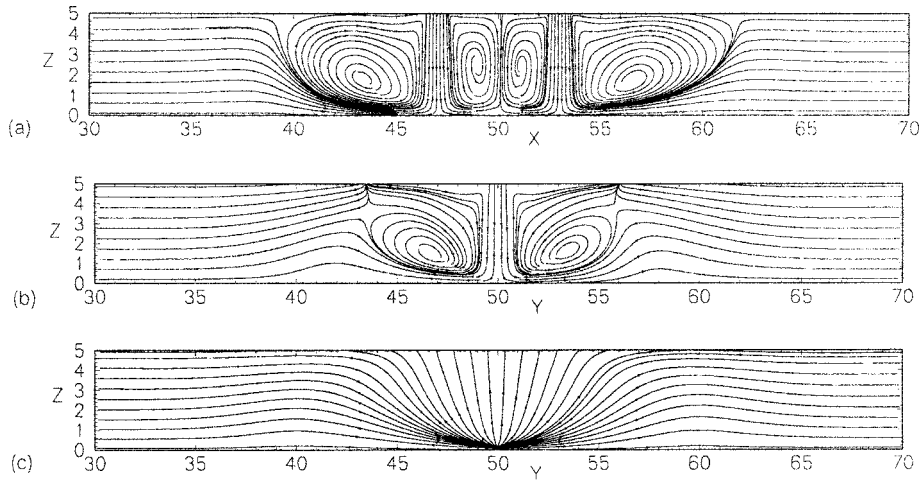


**Figure 2.** Stream trace plots for Re = 100, $A_z = 5$, and $X_n = 6$ on (*a*) mid *x*-*z* plane at $Y = 50$, (*b*) *y*-*z* plane at the center of the jet at $X = 47$, (*c*) mid *y*-*z* plane at $X = 50$.

squeezed between the jets and the fountain upwash flow, where its size is reduced considerably. Figure 2*b* shows the flow profile at the *y*-*z* plane corresponding to the center of one of the jets. The flow pattern at the mid *y*-*z* plane corresponding to the center of the upwash fountain is given in Figure 2*c*. Upon impingement of the upwash fountain on the top wall, an upper wall jet is formed, which spreads radially. The evolution of the entrainment vortex and wall jets is illustrated in Figure 3 through stream trace plots on different horizontal planes. The fluid is dragged radially toward the jets from the surrounding as soon as it exits from the nozzles. As a result a toroidal vortex is formed around each of the jets. Figure 3*a* corresponds to a horizontal plane where the upper wall jet is formed as the upwash fountain impinges on the top plate. Further downstream, at $Z = 2.5$, a wall jet forms in the *y*-direction (Figure 3*b*) as a result of jet impingement on the bottom plate. The wall jet along the *y*-direction is more prominent at a distance closer to the bottom plate (Figure 3*c*), and at $Z = 0.5$, the wall jets spreads radially outward (Figure 3*d*). The wall jets are separated from each other along the ground plane by stagnation lines or dividing lines everywhere equidistant from the two jet impingement centers, which contain a stagnation point. The separation of the wall jets by the stagnation lines also occurs in turbulent twin jets in practical V/STOL applications (Siclari et al. [27]). Figure 4 shows the stream traces on the midvertical *x*-*z* plane for $A_z = 1$ and Re = 300. For this rather low plate-to-plate distance the peripheral vortex around each jet is pushed toward the upper plate by the thickening wall jet. The formation of the peripheral vortices and the wall jets is illustrated in Figure 5 using the stream trace plots at different horizontal sections. A wall jet starts forming on the bottom plate along the *y*-direction with complex flow patterns as shown in Figure 5*b*. At elevations closer to the bottom plate, the flow pattern is characterized by the wall jets, which are separated from each other at the collision font (Figures 5*c* and 5*d*). A carpet plot of the vertical component of the velocity at the horizontal section at $Z = 0.3$ is shown in Figure 6. For this rather low plate-to-plate spacing the interaction of the jet with

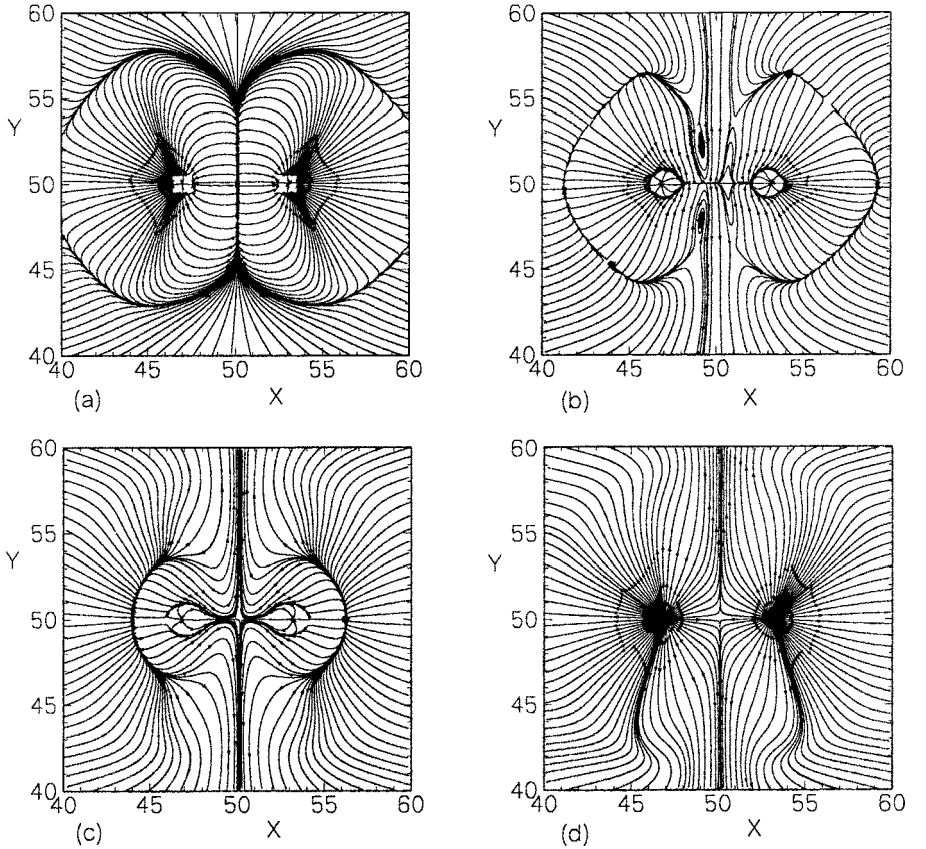


**Figure 3.** Stream trace plots for Re = 100, $A_z = 5$, and $X_n = 6$ at horizontal cross sections of (*a*) $Z = 4.75$, (*b*) $Z = 2.5$, (*c*) $Z = 1.5$, and (*d*) $Z = 0.5$.

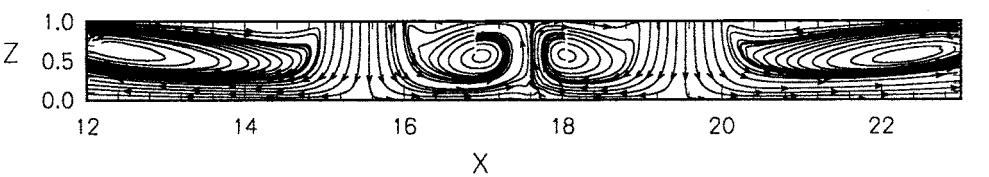


**Figure 4.** Stream trace plot on mid vertical $x$-$z$ plane for Re = 300, $A_z = 1$, and $X_n = 4$.

the lower plate produces four peaks at the four corners of each jet cross section. The off-center peaks of the jet velocity have also been observed in incompressible turbulent unbounded single jet flows issuing from rectangular nozzles by Sfeir [28], Tsuchiya et al. [29], and Quinn [30] and in laminar rectangular jet flows with small jet-to-wall distances (Sezai and Mohamad [7]). The variation of the vertical velocity component with vertical distance from the jet nozzles is shown in Figure 7. The

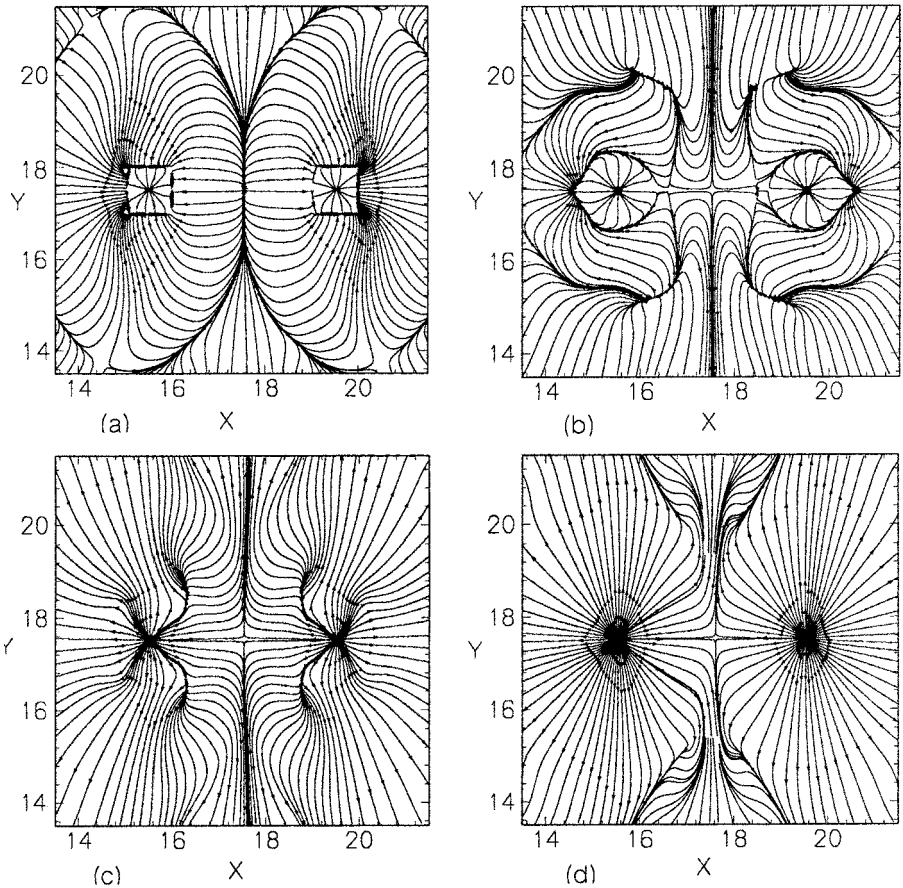


**Figure 5.** Stream trace plots for Re = 300, $A_z = 1$, and $X_n = 4$ at horizontal cross sections of (*a*) $Z = 0.95$, (*b*) $Z = 0.5$, (*c*) $Z = 0.3$, and (*d*) $Z = 0.1$.

off-center velocity peaks start forming at $Z = 0.7$. The difference between the peak and the jet center line velocity reaches a maximum at $Z = 0.5$ and then gradually levels off closer to the impingement plane.

At lower nozzle-to-plate spacings the upwash flow may disappear completely. Figure 8 shows the stream traces on the midvertical plane for a nozzle-to-plate spacing of $0.25D$. In a region close to the collision point of the two jets, the wall jet fills the whole gap between the plates. There is no recirculatory motion between the two jets at Re = 100 and 300 (Figures 8*a* and 8*b*), while at Re = 500 the vortex motion is confined in a very narrow space near the top plate (Figure 8c). Figure 9 shows the stream trace plots at different horizontal planes for $L_z/D = 0.25$ and Re = 500. At this low plate-to-plate spacing, a wall jet forms on both the top (Figure 9*a*) and the bottom plates (Figures 9*c* and 9*d*). The formation of two small counter-rotating vortices at the downstream side of each jet along the $x$-direction is apparent in Figure 9*b*. No off-center velocity peaks of the jet profile were found for nozzle-to-plate distance lower than 1.

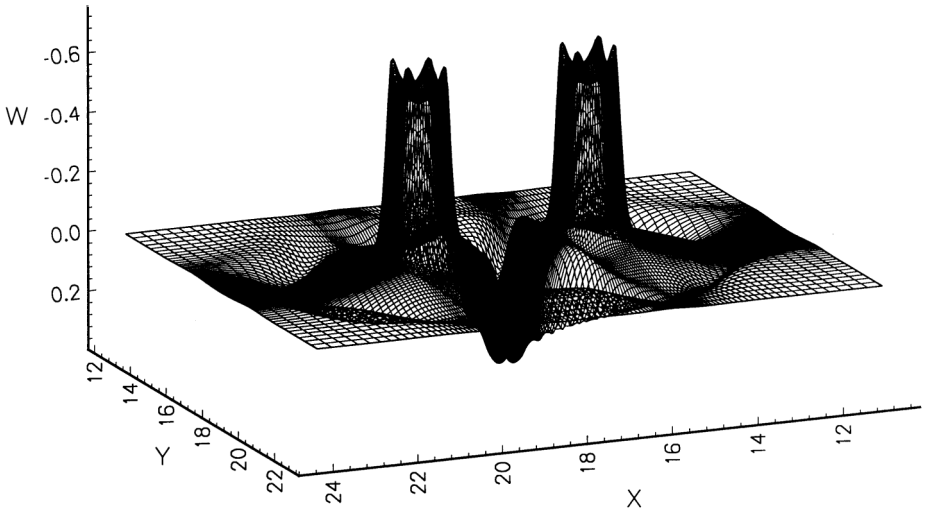


**Figure 6.** The three-dimensional plots of the $W$-velocity for Re = 300, $A_z = 1$, and $X_n = 4$ at the horizontal cross section, $Z = 0.3$.

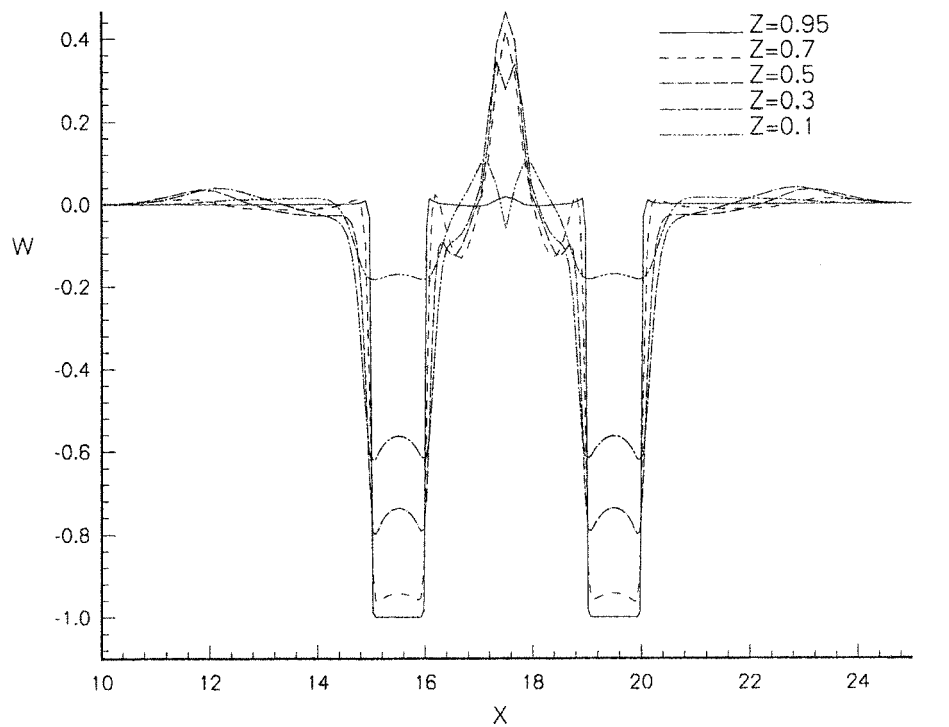


**Figure 7.** Variation of $W$-velocity with $X$ for Re = 300, $A_z = 1$, and $X_n = 4$ at different horizontal cross sections.

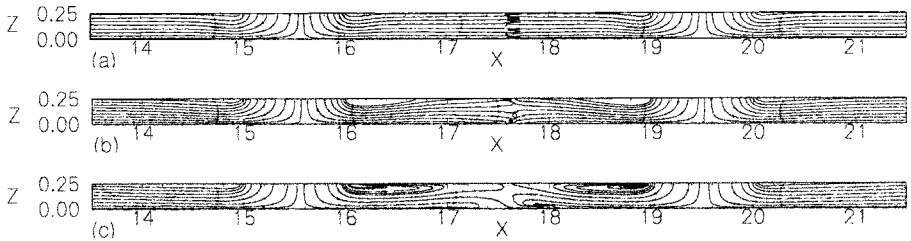


**Figure 8.** Stream trace plots on mid $x$-$z$ plane for, $A_z = 0.25$ and $X_n = 4$ for ($a$) Re = 100, ($b$) Re = 300, and ($c$) Re = 500.

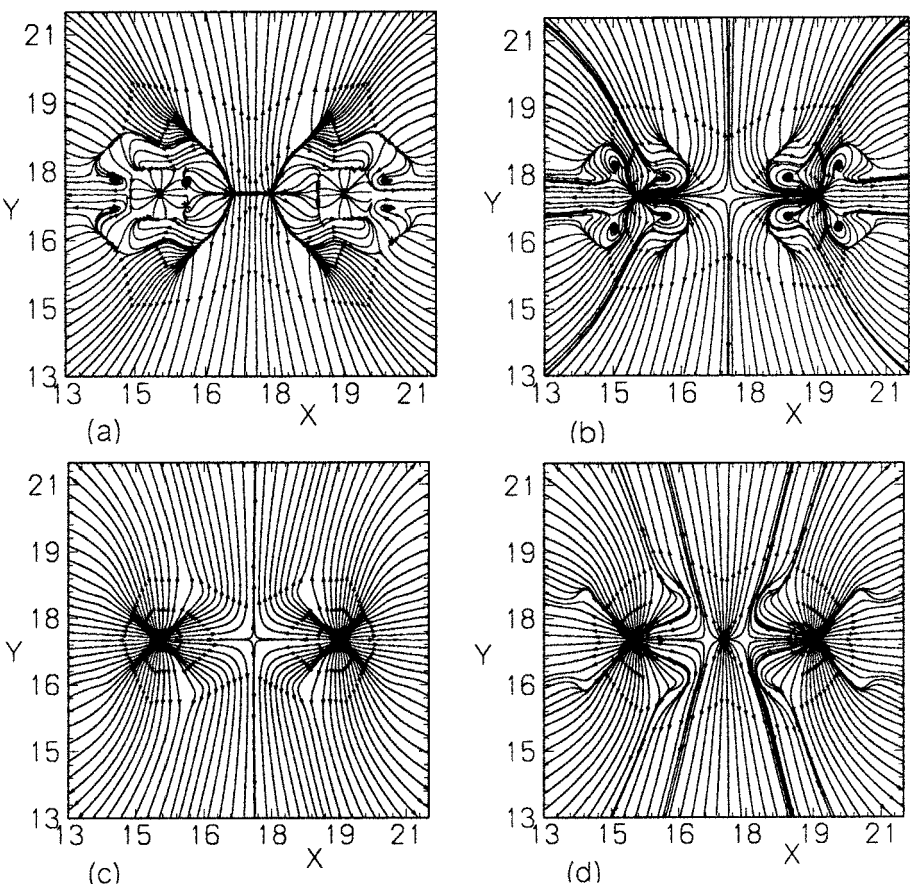


**Figure 9.** Stream trace plots for Re = 500, $A_z = 0.25$, and $X_n = 4$ on horizontal cross sections at ($a$) $Z = 0.225$, ($b$) $Z = 0.175$, ($c$) $Z = 0.075$, and ($d$) $Z = 0.0125$.

## Heat Transfer

The local convection heat transfer coefficient is defined as

$$h = \frac{q''_w}{t_w - t_j} \tag{6}$$

and the local Nusselt number is defined in terms of the jet width, $D$, as

$$\mathrm{Nu} = \frac{hD}{k} \tag{7}$$

where it is also equal to the nondimensional heat flux, $\mathrm{Nu}(x, y) = -\partial T/\partial Z|_{\mathrm{wall}}$ and calculated from $(T(i, j, 1) - T(i, j, 2)/\Delta Z)$ for a grid point $i, j$, on the bottom surface, where the vertical grid index $k$ is 1. Figure 10 shows the Nusselt number variation for Re = 300 and $A_z = 1$, corresponding to the jet velocity profile depicted in Figure 6. The four off-center peaks of Nusselt number for each jet are consistent with the jet velocity profile, which shows that the jet velocity distribution plays a significant role in impingement cooling. However, no such off-center peaks are observed for the rather small nozzle-to-plate distance of $L_z = 0.25D$ (Figure 11). The effect of jet-to-jet spacing, $X_n$, on the variation of local Nusselt number along the $x$-direction at the midsection is shown in Figure 12 for Re = 300 and $A_z = 2$. It is observed that the magnitude of the maximum Nusselt number is not affected by the jet-to-jet spacing, which may not be the case for an array of jets. Huber and Viskanta [16] found in their research on a $3 \times 3$ square turbulent jet array that the local Nusselt

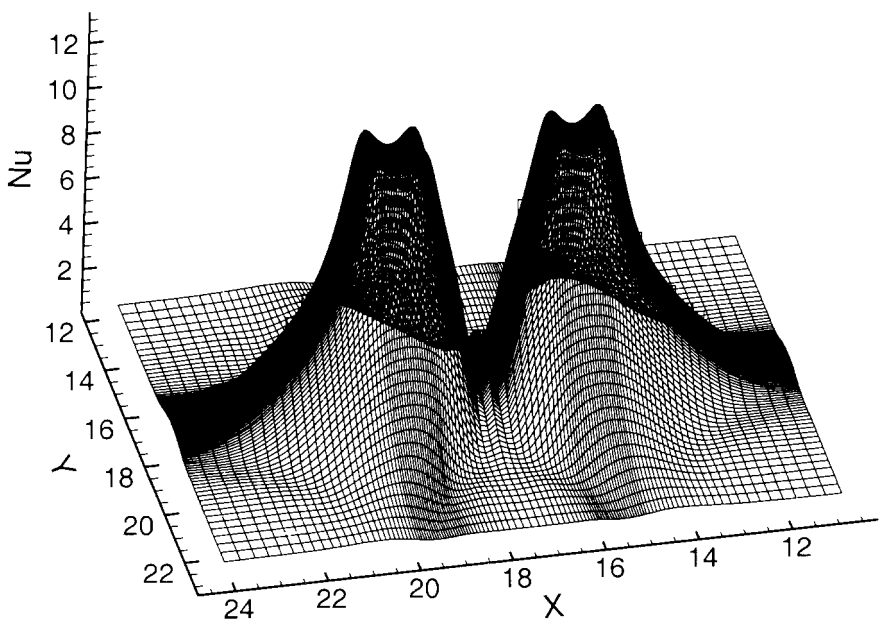


**Figure 10.** The three-dimensional plot of the Nusselt number for Re = 300, $A_z = 1$, and $X_n = 4$.

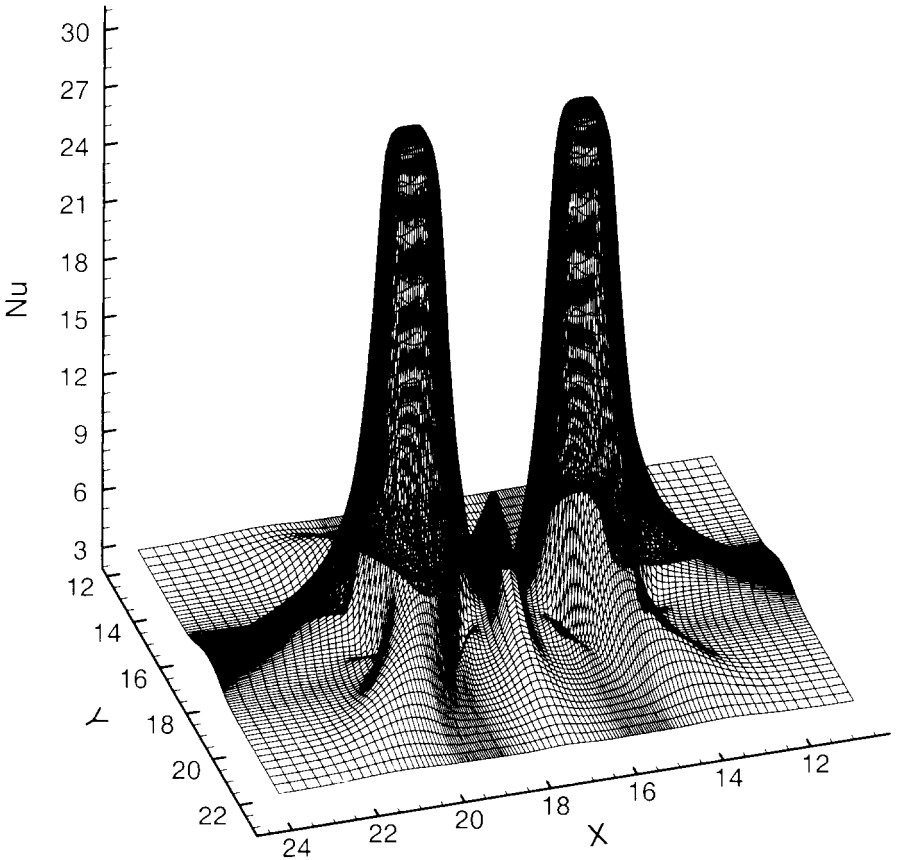


**Figure 11.** The three-dimensional plots of the Nusselt number for Re = 500, $A_z = 0.25$, and $X_n = 4$.

numbers for $X_n = 8$ are larger in magnitude than those obtained for $X_n = 6$ and $X_n = 4$ for $A_z = 1$ and 6. For all cases investigated in this article, the local Nusselt numbers at the stagnation points have been found to be less than those of single jets obtained by Sezai and Mohamad [7] by about 2%.

The effect of Reynolds number on the variation of local Nusselt number along the $x$-direction at the middle section ($Y = 17.5$) is shown in Figure 13 for $A_z = 1$ and $X_n = 6$. Heat transfer decreases sharply away from the jet axes. However, for Re = 500 there is a small jump in heat transfer at the midpoint between the jets. This is a result of the formation of the upwash fountain created by the colliding wall jets after impingement. The magnitude of the Nusselt number at the secondary stagnation point associated with the interaction between the opposing wall jets is expected to increase more when the Reynolds number is increased further. In fact, measurements by Slayzak et al. [8] indicate that the local convection coefficients in the interaction zone can be comparable with those associated with the jet impingement regions for turbulent jets. The effects of nozzle-to-plate spacing on the local Nusselt

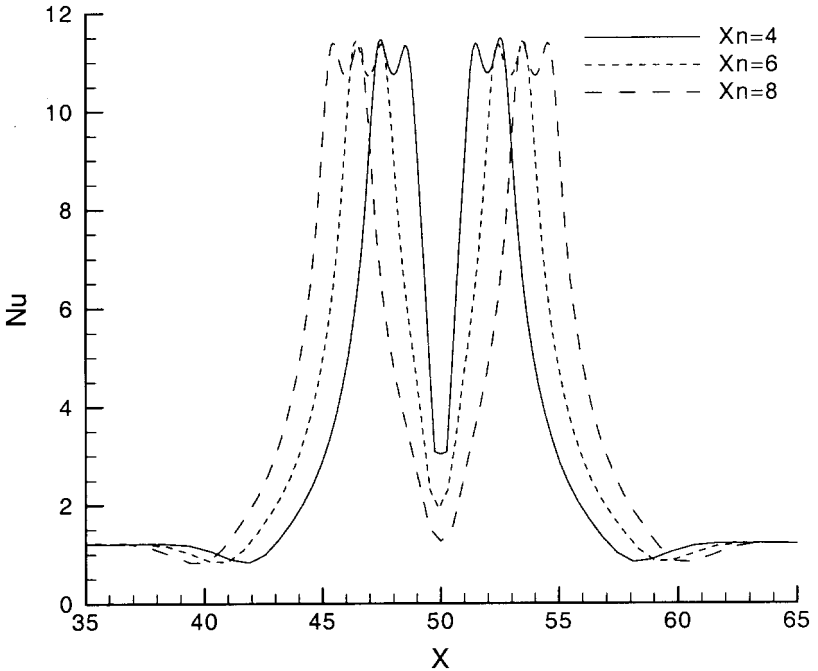


**Figure 12.** Effect of jet-to-jet spacing on Nusselt number variation for Re = 300, $A_z = 2$.

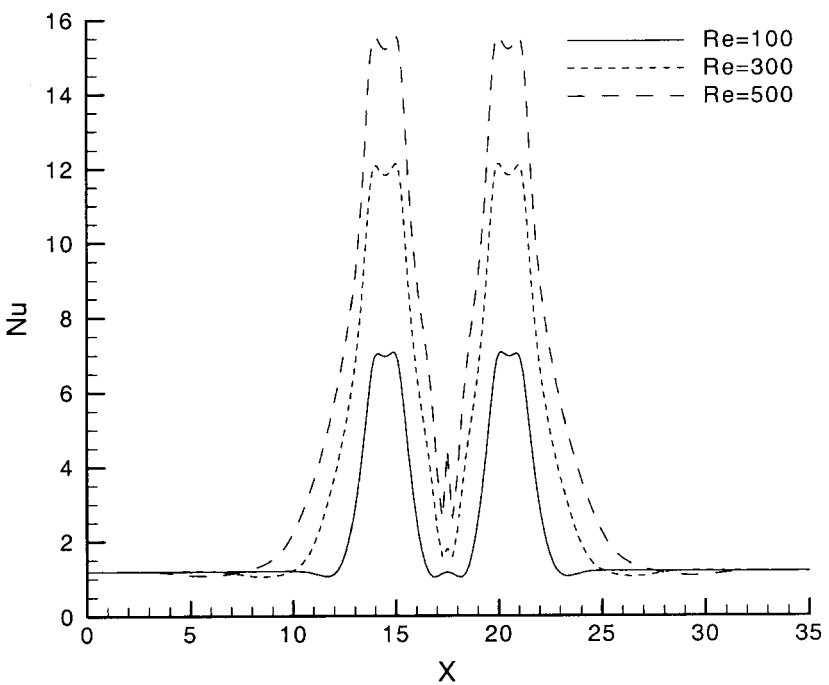


**Figure 13.** Effect of Reynolds number on local Nusselt number ($Y = 17.5$) for $A_z = 1$ and $X_n = 6$.

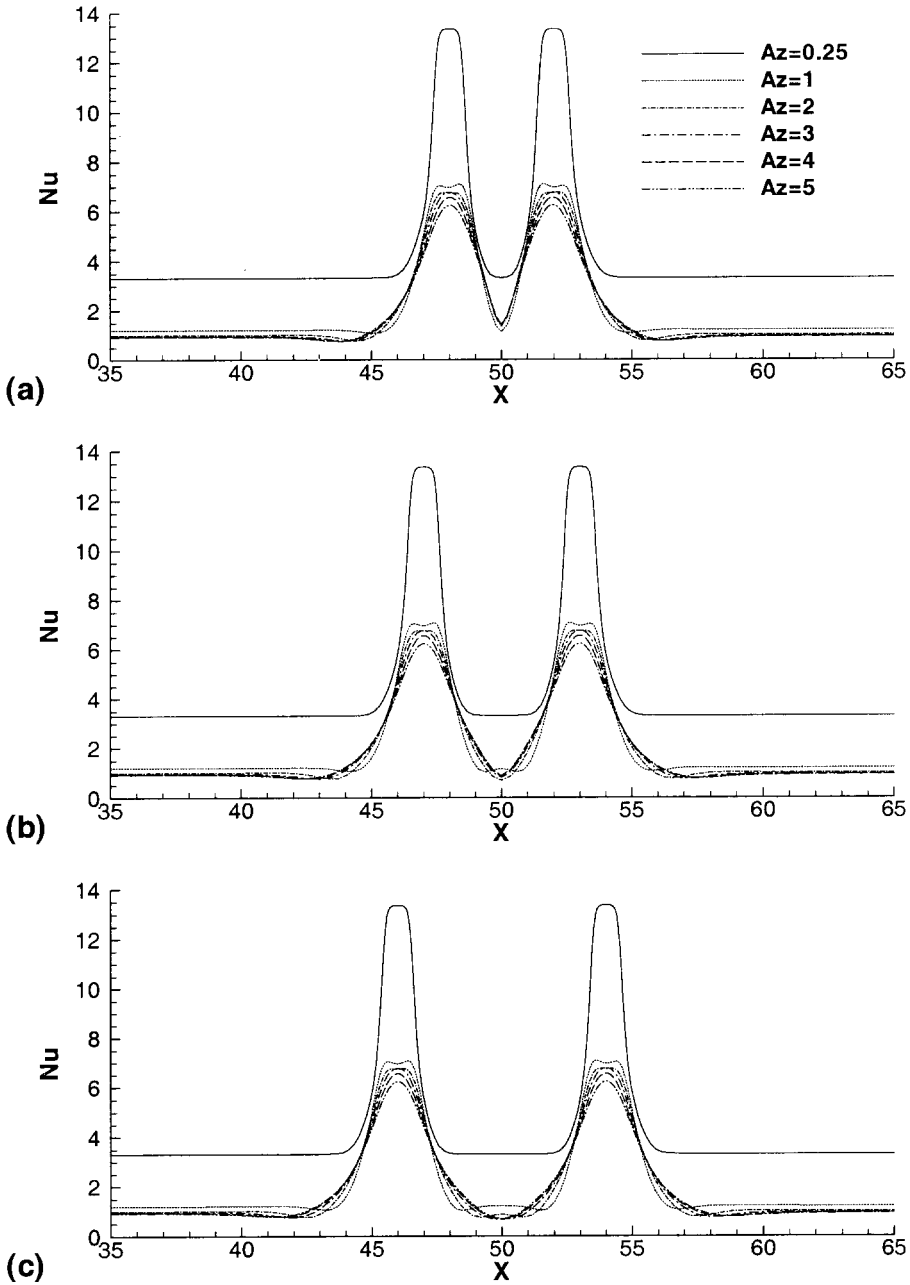


**Figure 14.** Effect of aspect ratio $A_z$ on Nusselt number variation in the $x$-direction for Re = 100 and different jet-to-jet spacing (*a*) $X_n = 4$, (*b*) $X_n = 6$, and (*c*) $X_n = 8$.

number along the $x$-direction at the middle section ($Y = 50$) for $\mathrm{Re} = 100$ are shown in Figure 14 for different jet-to-jet spacings. The stagnation Nusselt number increases as the nozzle-to-plate distance decreases. The rate of change in the stagnation Nusselt number is higher at closer nozzle-to-plate spacings. For the smallest nozzle-to-plate spacing investigated ($L_z \approx 0.25D$) the Nusselt number in the region far away from the impingement zone is much higher than that of the other nozzle-to-plate spacings due to the higher wall jet velocities attained.

## CONCLUSIONS

A three-dimensional numerical study has been undertaken to determine the flow and heat transfer characteristic of twin jets of square cross section. The results indicate a rather complex flow field with a peripheral vortex around each jet and an upwash fountain flow at the collision point of the jets. However, at very small nozzle-to-plate distances ($L_z \approx 0.25D$) no upwash fountain flow can form at the collision point where the jets are diverted along the transverse direction ($y$-direction). At this nozzle-to-plate distance wall jets may fill the whole plate-to-plate spacing so that no vortex motion can form around the jets. Unlike an array of jets, it has been found that the magnitude of the maximum Nusselt number is not affected by the jet-to-jet spacing. For a nozzle-to-plate spacing of one nozzle width the uniform jet velocity profile at the nozzle exit is transformed into a nonuniform profile having four off-center velocity peaks downstream of the nozzles. These peaks result in the formation of four off-center peaks in the Nusselt number profile at the impingement plate.

## REFERENCES

1. A. R. P. V. Heiningen, A. S. Majumdar, and W. J. M. Douglas, Numerical Prediction of the Flow Field and Impinging Heat Transfer Caused by a Laminar Slot Jet, *ASME Journal of Heat Transfer*, vol. 98, pp. 654–658, 1976.
2. Y. J. Chou and Y. H. Hung, Impingement Cooling of an Isothermally Heated Surface with a Confined Slot Jet, *ASME Journal of Heat Transfer*, vol. 116, pp. 479–482, 1994.
3. S. Mikhail, S. M. Morcos, M. M. M. Abou-Ellail, and W. S. Ghaly, Numerical Prediction of Flow Field and Heat Transfer from a Row of Laminar Slot Jets Impinging on a Flat Plat, *Proc. 7th Int. Heat Transfer Conf.*, vol. 3, pp. 337–382, 1982.
4. T. D. Yuan, J. A. Liburdy, and T. Wang, Buoyancy Effects on Laminar Impinging Jets, *Int. J. Heat Mass Transfer*, vol. 31, pp. 2137–2145, 1988.
5. D. M. Schafer, F. P. Incropera, and S. Ramadhyani, Numerical Simulation of Laminar Convection Heat Transfer from an In-Line Array of Discrete Sources to a Confined Rectangular Jet, *Numer. Heat Transfer, Part A*, vol. 22. pp. 121–141, 1992.
6. D. C. Wadsworth and I. Mudawar, Cooling of a Multichip Electronic Module by Means of Confined Two-Dimensional Jets of Dielectric Liquid, *ASME Journal of Heat Transfer*, vol. 112, pp. 891–898, 1990.
7. I. Sezai and A. A. Mohamad, 3-D Simulation of Laminar Rectangular Impinging Jets, Flow Structure and Heat Transfer, *ASME Journal of Heat Transfer*, vol. 121, pp. 50–56, 1999.
8. S. J. Slayzak, R. Viskanta, and F. P. Incropera, Effects of Interaction Between Adjacent Free Surface Planar Jets on Local Heat Transfer from the Impingement Surface, *Int. J. Heat Mass Transfer*, vol. 37, no. 2, pp. 269–282, 1994.
9. J. M. M. Barata, D. F. G. Durao, and M. V. Heitor, Impingement of Single and Twin Turbulent Jets through a Crossflow, *AIAA Journal*, vol. 29, no. 4, pp. 595–602, 1991.

10. S. H. Chuang, M. H. Chen, S. W. Lii, and F. M. Tai, Numerical Simulation of Twin-Jet Impingement on a Flat Plate Coupled with Cross-Flow, *Int. J. Numer. Meth. Fluids*, vol. 14, pp. 459–475, 1992.
11. S. H. Chuang and T. J. Nieh, Numerical Simulation and Analysis of Three-Dimensional Turbulent Impinging Square Twin-jet Flow Field with No-Crossflow, *Int. J. Numer. Meth. Fluids*, vol. 33, pp. 475–498, 2000.
12. M. J. Siclari, J. W. G. Hill, and R. C. Jenkins, Stagnation Line and Upwash Formation of Two Impinging Jets, *AIAA Journal*, vol. 19, pp. 1286–1293, 1981.
13. D. E. Metzger, L. W. Florschuetz, D. I. Takeuchi, R. D. Behee, and R. A. Berry, Heat Transfer Characteristic for Inline and Staggered Arrays of Circular Jets with Crossflow of Spent Air, *ASME Journal of Heat Transfer*, vol. 101, pp. 526–531, 1979.
14. B. R. Hollworth and L. Dagan, Arrays of Impinging Jets with Spent Fluid Removal through Vent Holes on the Target Surface—Part 1: Average Heat Transfer, *ASME J. Eng. Power*, vol. 102, pp. 994–999, 1980.
15. S. W. Kim and T. J. Benson, Fluid Flow of a Row of Jets in Crossflow—A Numerical Study, *AIAA Journal,* vol. 31, no. 5, pp. 806–811, 1993.
16. A. M. Huber and R. Viskanta, Effect of Jet-Jet Spacing on Convective Heat Transfer to Confined, Impinging Arrays of Axisymmetric Air Jets, *Int. J. Heat Mass Transfer*, vol. 37, no. 18, pp. 2859–2869, 1994.
17. J. M. M. Barata, Fountain Flows Produced by Multiple Impinging Jets in a Crossflow, *AAIA Journal*, vol. 34, no. 12, pp. 2523–2530, 1996.
18. K. Garrett and B. W. Webb, The Effect of Drainage Configuration on Heat Transfer Under an Impinging Liquid Jet Array, *ASME Journal of Heat Transfer*, vol. 121, pp. 803–810, 1999.
19. P. Y. Tzeng, C. Y. Soong, and C. D. Hsieh, Numerical Investigation of Heat Transfer Under Confined Impinging Turbulent Slot Jets, *Numer. Heat Transfer, Part A,* vol. 35, pp. 903–924, 1999.
20. S. H. Seyedein, M. Hasan, and A. S. Mujumdar, Laminar Flow and Heat Transfer from Multiple Impinging Slot Jets with an Inclined Confinement Surface, *Int. J. Heat Mass Transfer*, vol. 37, no. 13, pp. 1867–1875, 1994.
21. P. Leonard, A Stable and Accurate Convective Modelling Procedure Based on Quadratic Upstream Interpolation, *Comput. Method Appl. Mech. Engng.,* vol. 19, pp. 59–98, 1979.
22. B. P. Leonard and S. Mokhtari, Beyond First Order Upwinding: The ULTRA-SHARP Alternative for Nonoscillatory Steady-State Simulation of Convection, *Int. J. Numer. Methods Eng*., vol. 30, pp. 729–766, 1990.
23. B. P. Leonard and J. E. Drummond, Why You Should Not Use ''Hybrid,'' ''Power Law'' or Related Exponential Schemes for Convective Modelling. There Are Much Better Alternatives, *Int. J. Numer. Meth. Fluids*, vol. 20, pp. 421–442, 1995.
24. H. A. V. Van der Vorst, BICGSTAB: A Fast and Smoothly Converging Variant of Bi-CG for the Solution of Non-Symmetric Linear Systems, *SIAM J. Sci. Statist. Comput*., vol. 10, pp. 1174–1185, 1989.
25. Y. Saad, *Iterative Methods for Sparse Linear Systems*, PSW Publ. Co., Boston, 1996.
26. J. P. Van Doormaal and G. D. Raithby, Enhancements of the SIMPLE Method for Predicting Incompressible Fluid Flows, *Numer. Heat Transfer*, vol. 7, pp. 147–163, 1984.
27. M. J Siclari, D. Migdal, and J. L. Palcza, The Development of Theoretical Models for Jet-Induced Effects on V/STOL Aircraft, *Journal of Aircraft*, vol. 13, pp. 938–944, 1976.
28. A. Sfeir, Investigation of Three-Dimensional Turbulent Rectangular Jets, *AIAA Journal*, vol. 17, pp. 1055–1060, 1979.
29. Y. Tsuchiya, C. Horikoshi, and T. Sato, On the Spread of Rectangular Jets, *Exp. Fluids*, vol. 4, pp. 1197–1204, 1986.
30. W. R. Quinn, Passive Near-Field Mixing Enhancement in Rectangular Jet Flows, *AIAA Journal*, vol. 29, pp. 515–519, 1991.